

See discussions, stats, and author profiles for this publication at: <https://www.researchgate.net/publication/231665795>

Solvation of Cu^{2+} in Water and Ammonia. Insight from Static and Dynamical Density Functional Theory

ARTICLE · NOVEMBER 1999

CITATIONS

23

READS

9

1 AUTHOR:



Attila Bérces

Omixon

67 PUBLICATIONS 1,621 CITATIONS

SEE PROFILE

Solvation of Cu^{2+} in Water and Ammonia. Insight from Static and Dynamical Density Functional Theory

Attila Bérces*

Steacie Institute for Molecular Sciences, 100 Sussex Drive, Ottawa, K1A 0R6, Canada

Tomoo Nukada

The Institute of Physical and Chemical Research (RIKEN), Wako-shi, Saitama, 351, Japan

Peter Margl† and Tom Ziegler

Department of Chemistry, The University of Calgary, Calgary, Alberta T2N 1N4, Canada

Received: July 27, 1999

We have studied the solvation of divalent copper by water and ammonia through the optimization of the structures of $[\text{Cu}(\text{H}_2\text{O})_n]^{2+}$ and $[\text{Cu}(\text{NH}_3)_n]^{2+}$, $n = 3-8$, by static density functional theory and ab initio molecular dynamics simulations. We found that as the number of solvent molecules increases to more than four, the additional ligands prefer to be hydrogen-bonded to the planar tetragonal primary hydration shell of $[\text{Cu}(\text{solvent})_4]^{2+}$ instead of filling the vacant axial position. The energetic preference of water is about 20–35 kJ/mol for the hydrogen bond compared to the axial position, whereas ammonia shows preference of only a few kJ/mol. Dynamical simulations were successful in reaching the lowest energy conformations. Especially remarkable is the dynamics of $[\text{Cu}(\text{H}_2\text{O})_8]^{2+}$, which has evolved from an eight-coordinate structure to a planar structure with four primary and four secondary solvent molecules in a short 10 ps simulation. Both $[\text{Cu}(\text{H}_2\text{O})_8]^{2+}$ and $[\text{Cu}(\text{NH}_3)_8]^{2+}$ prefer a quasi-planar structure with a total of eight hydrogen bonds between the solvent molecules in the first and second solvation shells. Each secondary water and ammonia is hydrogen-bonded to two adjacent molecules in the primary solvation shell. It is remarkable that ammonia can form two hydrogen bonds with only one lone electron pair. The strong network of hydrogen bonds stabilizes the tetragonal planar primary hydration shell. These calculations indicate that the high kinetic stability of the eight-coordinate clusters in previous mass spectrometry experiments is related to the stabilization of the planar primary solvation shell by the network of hydrogen bonds. We found a correlation between experimental ion signals in the gas phase and the planarity of the first solvation shells.

Introduction

The preferred number of coordinating ligands and the coordination geometry exhibit a large diversity for metal ions. The number of coordinating ligands ranges from four to nine, and each coordination number has more than one corresponding solvent structure. These coordination preferences often play a significant role in the biological functions of metal-containing enzymes. The metal-specific binding sites of proteins achieve their selectivity by providing a coordination environment preferred by only one element naturally found in the living systems. Some metals that are not naturally occurring in the food chain owe their toxicity to their ability to coordinate strongly in the binding sites of biologically important metals.¹ The release and capture of metal ions at the metal binding site are also controlled by a mechanism that changes the coordination environment between strongly and weakly binding coordination modes. The coordination site of calcium-binding enzyme calmodulin has the ability to eliminate calcium when it is no longer needed by changing the geometry of the binding site.²

Solvation studies of metal ions often give insight into the preferred coordination modes of metals in biological systems.

Some metals have a strong energetic preference for a particular coordination mode, while other metals can assume more diverse coordination structures without a large energetic penalty. At one end of the spectrum of coordination modes is the divalent calcium, which is most often coordinated to six to nine ligands and has a strong preference for oxygen donors. Including the substrate, calcium is coordinated to eight ligands in the crystal structure of the C-type mannose binding protein complexed with an oligosaccharide.³ Ab initio calculations have shown that the net energy penalty for changing the number of water molecules in the primary solvation shell of divalent calcium between six to eight is very small, which is consistent with its coordination preferences in biological systems.⁴

Ab initio calculations have shown that divalent beryllium prefers a tetrahedral coordination of water molecules⁵ while divalent magnesium prefers octahedral coordination.⁶ The energetic preference of beryllium and magnesium between the tetrahedral and octahedral alternatives is as much as 22 and 34 kcal/mol, respectively. In contrast, the ab initio energies of $\text{Zn}[\text{H}_2\text{O}]_4^{2+} \cdot 2\text{H}_2\text{O}$, $\text{Zn}[\text{H}_2\text{O}]_5^{2+} \cdot \text{H}_2\text{O}$, and $\text{Zn}[\text{H}_2\text{O}]_6^{2+}$ differ by less than 1 kcal/mol⁷ and the preferred coordination depends on the chosen conditions.⁸ The solvation of divalent zinc by ammonia does not show a clear energetic preference for

† Current address: Eastman Chemical Company, Building 150B, Lincoln Street, Kingsport, TN 37662-5150.

octahedral or tetrahedral coordination, similar to the divalent zinc–water clusters.⁹

Recent experimental measurements of the incremental binding energies of water to divalent metal ions has shown that Ni^{2+} has a much larger binding energy for the sixth water than for any additional ones, indicating its preference for six-coordination. The same experiment was not conclusive regarding the coordination of divalent calcium to water.¹⁰

Zinc, nickel, and alkaline earth metals have been extensively studied both by experimental and theoretical methods. On the other hand, divalent copper has been an unsolved challenge experimentally until recently. Stace and co-workers have succeeded in producing doubly charged copper coordinated to solvent molecules in the gas phase and studied the distribution of these ions by mass spectrometry.^{11,12} The distribution of the ion intensity as a function of the number of solvent molecules gives insight into structures of metal–solvent complexes. Many of these measurements showed correlation between the most intense ion signal and the primary solvation unit in solution phase.^{13–17} The experiments of Stace and co-workers found that Cu^{2+} complexed to water, ammonia, and methanol have shown maximum intensity for the eight-coordinated clusters.^{11,12} These data imply that the six-coordinated metal–solvent complexes, $[\text{Cu}(\text{H}_2\text{O})_6]^{2+}$ and $[\text{Cu}(\text{NH}_3)_6]^{2+}$, are not the most stable forms in the gas phase and may not be the primary solvation units as it is most often assumed.¹⁸ Calcium can accommodate eight water molecules in its first hydration shell; thus, the possibility of coordination by eight solvent molecules would not be unprecedented. However, the ionic radius of copper is smaller than that of calcium and the most common coordination number of copper is four, five, or six. There is also some uncertainty about the relationship between solvent shell development and ion intensity distribution in the mass spectrum. Considering the strong energetic preferences of certain metals for a given coordination mode, the correlation between the most intense ion signal in the mass spectrum and the primary solvation unit can be rationalized. However, since these measurements do not correspond to equilibrium conditions, this empirically found correlation has not been clearly understood. The intriguing results of Stace et al. have prompted us to carry out molecular modeling of $[\text{Cu}(\text{H}_2\text{O})_n]^{2+}$ and $[\text{Cu}(\text{NH}_3)_n]^{2+}$, $n = 3–8$, based on density functional theory (DFT). We are interested in determining the structures of the clusters, in particular with eight solvent molecules, which may shed light on the outstanding intense signal these clusters produce in the mass spectrometry experiments.

The number of different coordination modes and conformations can reach several hundred for the largest system of this study. The large variety of possible structures poses a problem for theoretical calculations, since it is difficult to tell *a priori* which conformations are worth studying. Car–Parrinello molecular dynamics¹⁹ (CPMD) offers an alternative for finding the most energetically preferred conformation by constant temperature molecular dynamics simulations. Parrinello^{20,21} and Klein^{22,23} and their co-workers used CPMD to study solvated metal ions. As long as the barrier between the starting conformation and the lowest energy conformation is not too high, the dynamical trajectory will populate the lowest energy conformations after a long enough simulation time. These dynamical simulations are limited to about 10 ps for the systems of our interest, which is too short to find the most stable conformation by starting from any randomly selected conformation. For this reason, we used a combination of geometry optimization by static density functional method and Car–Parrinello molecular dynamics to

study the most stable coordination modes of $[\text{Cu}(\text{H}_2\text{O})_n]^{2+}$ and $[\text{Cu}(\text{NH}_3)_n]^{2+}$, $n = 3–8$. In this study we describe the optimized geometries and energies of these divalent copper–solvent clusters with particular emphasis on comparing alternative structures with different numbers of solvent molecules in the primary solvation shell. Our most extensive dynamical study was of the conformations of $[\text{Cu}(\text{H}_2\text{O})_8]^{2+}$, which we discuss in detail.

Computational Details

Static DFT Calculations. The reported static calculations were carried out with the Amsterdam Density Functional (ADF) program system, version 2.3, derived from the work of Baerends et al.²⁴ and developed at the Free University of Amsterdam^{25–27} and at the University of Calgary.^{28–32} All optimized geometries calculated in this study are based on the local density approximation³³ (LDA) augmented with gradient corrections to the exchange³⁴ and correlation³⁵ potentials. These calculations include quasi-relativistic corrections to the Hamiltonian introduced by Snijders et al.³⁶ Schreckenbach et al. have implemented the analytic energy gradients of the quasi-relativistic corrections.³⁷ All open-shell calculations were spin-unrestricted.

The atomic orbitals on copper were described by an uncontracted triple- ζ Slater function basis set,³⁸ while a double- ζ Slater function basis set was used for nitrogen, oxygen, and hydrogen; a single- ζ polarization function was used on all atoms. The $1s^2$ configuration of nitrogen and oxygen and the $1s^2 2s^2 2p^6$ configuration of copper were assigned to the core and treated by the frozen-core approximation.²⁴ The electron density was fitted to a set of s, p, d, f, g, and h Slater functions centered on all nuclei to calculate the Coulomb and exchange potentials accurately in each SCF cycle.³⁹ Gradient-corrected DFT calculations were repeatedly shown to provide exceptionally good energetics for transition metal systems.⁴⁰

Dynamical DFT Calculations. Dynamical DFT calculations were carried out with the projector augmented wave (PAW) method of Blöchl,⁴¹ which is an implementation of the Car–Parrinello type *ab initio* molecular dynamics.¹⁹ All PAW calculations were spin-unrestricted. Carloni, Blöchl, and Parrinello applied PAW to calculate the spin splitting of a $\text{Cu}(\text{II})$ complex that has an electronic structure similar to that of the four-coordinate solvent clusters described in this paper.⁴² This method uses an augmented plane wave basis set that allows us to describe the full all-electron wave function. The description of the core wave function takes advantage of the frozen core approximation. The plane wave energy cutoff is 30 Ry in the present calculations. Periodic boundary conditions were used with a unit cell defined by lattice vectors $([0.0\ 10.0\ 10.0]\ [10.0\ 0.0\ 10.0]\ [10.0\ 10.0\ 0.0])$ Å. All calculations employed the exchange correlation functional of the generalized gradient approximation with the local potential of Perdew and Zunger⁴³ augmented by the gradient corrections to the exchange and correlation of Becke and Perdew. To prevent electrostatic interactions between periodic images, a charge isolation scheme is used.⁴⁴ To achieve an evenly distributed thermal excitation, the nuclei were brought to a temperature of 300 K by applying a sequence of 50–150 sinusoidal pulses of excitation vectors orthogonal to the already excited modes. A temperature of 300 K was maintained for all simulations by a Nosé thermostat,^{45,46} which creates a canonical (*NVT*) ensemble. The fictitious kinetic energy of the electrons was controlled in a similar fashion by a Nosé thermostat.⁴⁷ To span large portions of configuration space in a minimum of time, the true masses of the nuclei were rescaled to 5.0 (Cu), 2.0 (O and N), and 1.5 (H) amu. Together

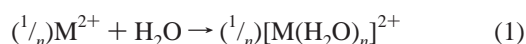
TABLE 1: Symmetry, Electronic State, Average Binding Energy (kJ/mol), and Sequential Binding Energy (kJ/mol) of [Cu(H₂O)_n]²⁺

| conformer | symmetry | electronic state | average BE | sequential BE | relative energy |
|-----------|-----------------|------------------|------------|---------------|-----------------|
| 1a | C _s | 2A' | 380 | | 0 |
| 1b | C _s | 2A' | 380 | | 1 |
| 1c | C _{2v} | 2A ₁ | 377 | | 9 |
| 2a | C ₁ | 2A | 329 | 175 | 0 |
| 2b | C ₁ | 2A | 329 | 175 | 0 |
| 2c | C _s | 2A' | 328 | 174 | 1 |
| 2d | C ₁ | 2A | 327 | 170 | 5 |
| 2e | C _{2v} | 2A ₁ | 324 | 155 | 20 |
| 2f | C _{2v} | 2A ₁ | 320 | 142 | 33 |
| 3a | C ₁ | 2A | 292 | 144 | 0 |
| 3b | C ₁ | 2A | 284 | 107 | 37 |
| 3c | C ₁ | 2A | 284 | 105 | 39 |
| 4a | C ₁ | 2A | 263 | 122 | 0 |
| 4b | C _i | 2A _g | 262 | 109 | 13 |
| 4c | C ₁ | 2A | 259 | 93 | 29 |
| 4d | C ₁ | 2A | 251 | 51 | 71 |
| 5a | C ₁ | 2A | 242 | 116 | 0 |
| 5b | C ₁ | 2A | 234 | 51 | 65 |
| 5c | C ₁ | 2A | 230 | 28 | 88 |
| 5d | C ₁ | 2A | 228 | 15 | 101 |
| 6a | C ₁ | 2A | 224 | 99 | 0 |
| 6b | C _{2h} | 2A _g | 223 | 86 | 13 |
| 6c | C ₁ | 2A | 222 | 76 | 23 |
| 6d | C ₂ | 2A | 189 | N/A | 285 |

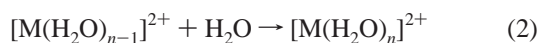
with an integration time step of 7 au (0.17 fs), this choice ensures good energy conservation during the dynamics simulation without computational overhead due to heavy atomic nuclei. Since we do not discuss time-dependent properties and since configurational ensemble averages remain unchanged under a rescaling of the masses, this technique is appropriate. Since the nuclear velocities scale with $m^{-1/2}$, the sampling is sped up by a factor of 1.5–2.

Results

The structures of various isomers of [Cu(H₂O)_n]²⁺ and [Cu(NH₃)_n]²⁺ clusters are shown in Figures 1 and 2, respectively. These figures include some of the most significant interatomic distances, the Cu–N bond lengths, the length of hydrogen bonds, and in some cases some nonbonded distances that are important for the interpretation of the figures. Bending angles in these figures normally refer to O–Cu–O bending angles where the two oxygen are in the trans position unless it is clearly marked otherwise. The binding energies and sequential binding energies of [Cu(H₂O)_n]²⁺ are listed in Table 1 and those of [Cu(NH₃)_n]²⁺ in Table 2. The average binding energies were calculated on the basis of the reaction energy corresponding to



The incremental binding energies correspond to the reaction energy of



where the most stable isomer of the $n - 1$ cluster is taken as a reference unless otherwise stated in the text. Zero-point corrections were not determined, since these require calculations of vibrational frequencies, which is prohibitively expensive for the largest clusters. There are different notations in the literature for distinguishing between the different binding modes of solvent–metal clusters. The “ $n + m$ ” notation refers to n solvent molecules in the primary solvation shell and m solvents in the

TABLE 2: Symmetry, Electronic State, Average Binding Energy (kJ/mol), and Sequential Binding Energy (kJ/mol) of [Cu(NH₃)_n]²⁺

| conformer | symmetry | electronic state | average BE | sequential BE | relative energy |
|------------|-----------------|-----------------------------|------------|---------------|-----------------|
| 7a | C _s | 2A' | 478 | | 0 |
| 8a | C _{2v} | ² A ₁ | 405 | 188 | 0 |
| 8b | C ₁ | 2A | 405 | 188 | 0 |
| 8c | C ₂ | 2A | 405 | 187 | 1 |
| 8d | C ₁ | 2A | 404 | 183 | 5 |
| 8e | C _s | 2A' | 404 | 183 | 5 |
| 8f | C _{2v} | 2A | 404 | 182 | 6 |
| 9a | C ₁ | 2A | 344 | 97 | 0 |
| 9b | C ₁ | 2A | 343 | 95 | 2 |
| 9c | C ₁ | 2A | 343 | 95 | 2 |
| 9d | C ₁ | 2A | 343 | 93 | 4 |
| 10a | C ₁ | 2A | 302 | 95 | 0 |
| 10b | C ₁ | 2A | 301 | 89 | 6 |
| 10c | C ₁ | 2A | 301 | 89 | 6 |
| 10d | C ₁ | 2A | 295 | 58 | 37 |
| 10e | C ₁ | 2A | 284 | −8 | 103 |
| 11a | C ₁ | 2A | 270 | 76 | 0 |
| 11b | C ₁ | 2A | 268 | 61 | 15 |
| 11c | C ₁ | 2A | 262 | 17 | 59 |
| 11d | C ₁ | 2A | 261 | 10 | 66 |
| 11e | C ₁ | 2A | 256 | −19 | 95 |
| 12a | C ₁ | 2A | 245 | 74 | 0 |
| 12b | C ₁ | 2A | 245 | 69 | 5 |
| 12c | C ₁ | 2A | 244 | 64 | 10 |
| 12d | C ₁ | 2A | 234 | −15 | 89 |
| 12e | C ₁ | 2A | 234 | −21 | 95 |
| 12f | C ₁ | 2A | 201 | N/A | 355 |

secondary shell. The same structure is sometimes referred to as M[S]_n²⁺·mS where M is the metal and S is the solvent.

The interaction of the doubly charged copper ion with water or ammonia is mainly an electrostatic charge–dipole interaction. The water molecules are oriented with one of the two lone pairs on the oxygens pointing in the direction of the Cu–O bond. The Cu²⁺ cluster with three water molecules assumes an essentially planar trigonal structure (**1a–1c**) with significant distortion from the regular triangle. The rotation of one water fragment around the Cu–O bond does not change the energy significantly. However, restricting the geometry of the oxygen, copper, and two hydrogens in the same plane (i.e., **1c**) raises the energy by 9 kJ/mol. The addition of the fourth water molecule yields some planar (**2a**, **2c**, and **2d**) and some nonplanar (**2b**, **2f**, and **2e**) conformations. The two most stable conformations of [Cu(H₂O)₄]²⁺, **2a** and **2b**, are essentially isoenergetic and planar. The tetrahedrally distorted isomer (**2b**) has the trans water molecules in a bent position characterized by 170° O–Cu–O bending angles. The planar conformation (**2a**) has one of the trans oxygen pairs in a near-linear arrangement, while the other trans ligand pair is bent but remains in the plain and is characterized by a 171° O–Cu–O bending angle. The O–Cu–O bending angle close to 170° is a recurring feature in many of the larger clusters. In the two most favorable conformations, the oxygen lone pairs are staggered (gauche) with respect to the neighboring copper–oxygen bonds to minimize bond–lone pair repulsion. A large number of different conformations are possible depending on the relative orientation of the water molecules. Structures with the hydrogens on the trans oxygen atoms in staggered positions have the highest energy.

The fifth and any additional water molecules can assume either an axial position (**3b**) or a hydrogen-bonded position to one or two of the water molecules in the first hydration shell (**3a**). The most energetically preferred position is the double-hydrogen-bonded position where the two lone pairs of the fifth

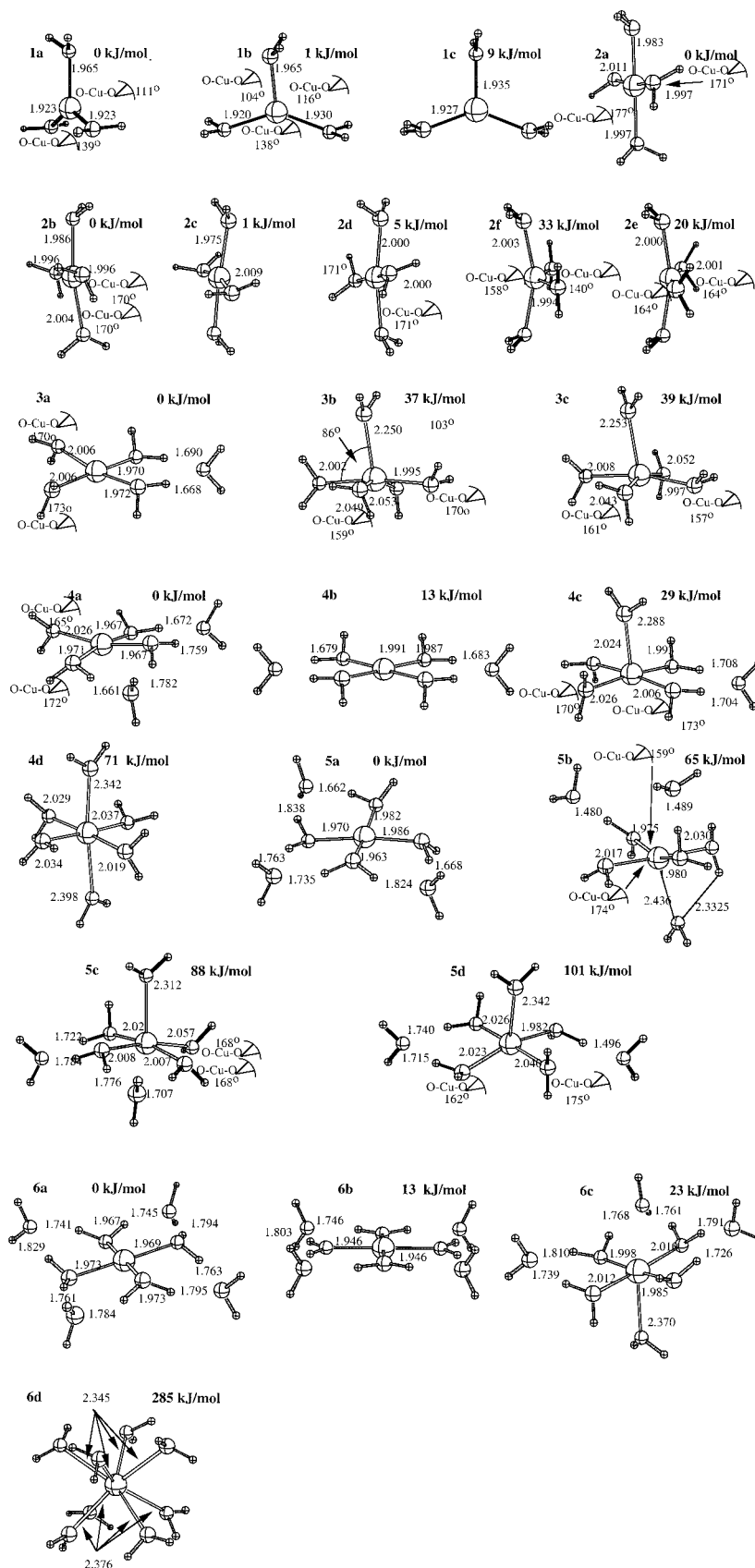


Figure 1.

ligand are directed toward the hydrogen atoms of two adjacent water molecules of the first hydration shell (**3a**). This double hydrogen bond is characterized by a binding energy of 144 kJ/mol and hydrogen bond lengths of 1.67 and 1.69 Å. The water molecules of the first hydration shell are highly polarized, which

is responsible for the unusually large strength of these hydrogen bonds. The binding energy of the fifth water molecule to the axial position in tetragonal planar geometry is 107 kJ/mol, which is 37 kJ/mol less favorable compared to the energy of the double hydrogen bond. Binding in the axial position (**3b** and **3c**) further

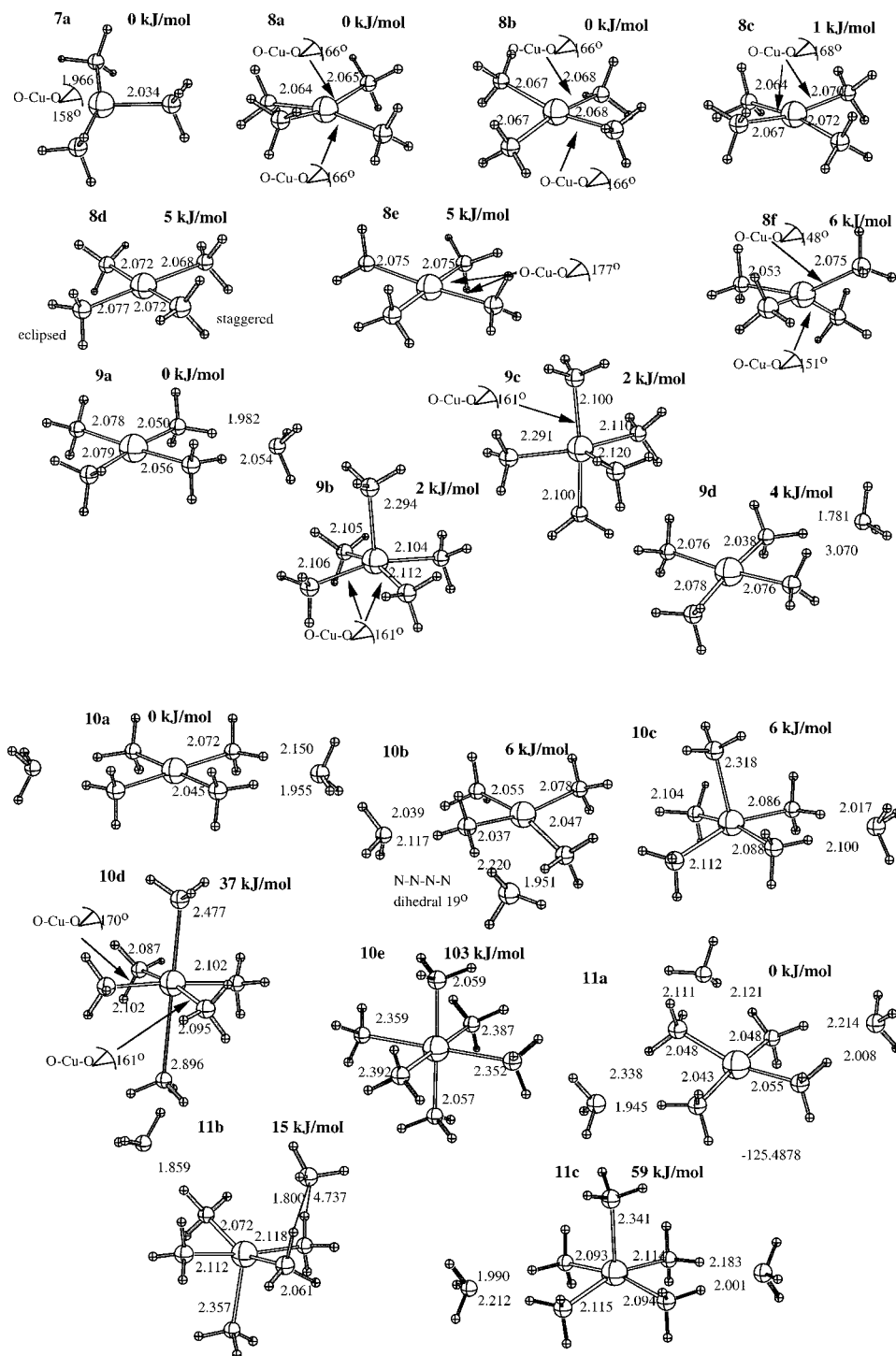


Figure 2.

distorts the trans O—Cu—O bending angle from linearity to about 160° . On the other hand, the double hydrogen bond (**3a**) ensures a near-planar structure for the four water molecules of the primary hydration shell.

$[\text{Cu}(\text{H}_2\text{O})_6]^{2+}$ can assume structures with four (**4a**, **4b**), five (**4c**), or all six (**4d**) ligands in the primary hydration shell. The lowest energy structure (**4a**) has four water molecules directly bonded to copper, and two water molecules are doubly hydrogen-bonded to the water in the primary hydration shell. There is an energetic preference for the structure with the two hydrogen-bonded water molecules on two adjacent sides of the tetragonal frame (**4a**). This structure allows for one of the water molecules to be somewhat distorted from the plane. On the other

hand, the conformation with two hydrogen-bonded water molecules on opposite sides of the tetragonal frame (**4b**) has higher energy by 13 kJ/mol. This energetic cost is likely related to the planar structure of the first hydration shell, which is not as favorable as the nonplanar. The sequential water binding energy is 122 kJ/mol in the hydrogen-bonded position (**4a**) and 93 kJ/mol in the axial position directly bonded to Cu (**4c**). The octahedral structure with all six water molecules in the primary hydration shell (**4d**) is 71 kJ/mol higher in energy than the most stable conformation. The local geometry around the copper is distorted from octahedral to tetragonal bipyramidal with the axial bonds being $0.3\text{--}0.4\text{ \AA}$ longer than those in the equatorial position.

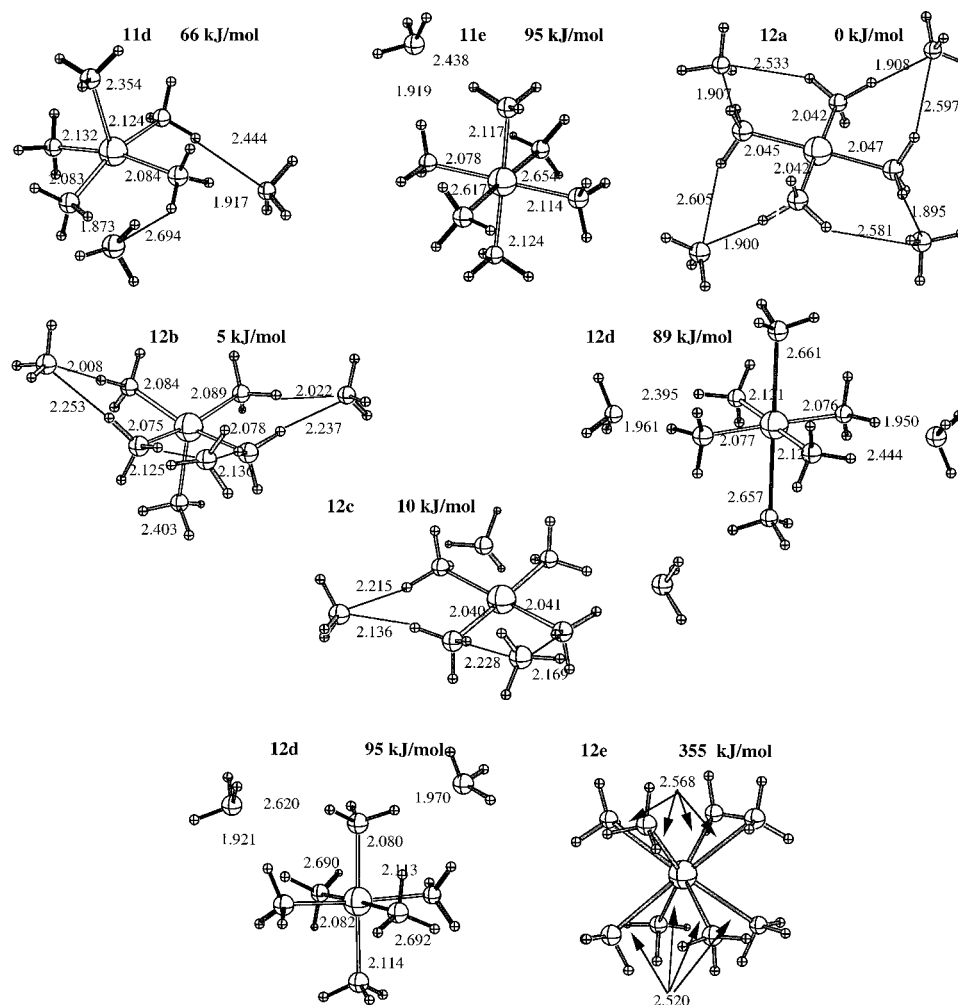


Figure 2. Continued.

The sequential binding energy of the seventh water molecule in the doubly hydrogen-bonded position is 116 kJ/mol with a corresponding structure for all water molecules in the same plane (**5a**). The structure derived from the most stable conformation of $[\text{Cu}(\text{H}_2\text{O})_6]^{2+}$ by adding one water molecule into the axial position (**5c**) is 88 kJ/mol above the most stable structure and represents only 26 kJ/mol sequential binding energy for the axial water molecule. Another structure with a water molecule in the axial position (**5d**) is 101 kJ/mol above the most stable conformation with a corresponding sequential binding energy of only 15 kJ/mol. In this structure one of the water molecules in the outer shell is bound by a single hydrogen bond to the water in the primary shell. An unusual structure (**5b**) has one of the water molecules partly bonded to the metal in the axial position and partly hydrogen-bonded to one of the first hydration shell water molecules.

We have tried to optimize $[\text{Cu}(\text{H}_2\text{O})_8]^{2+}$ with all eight water molecules in the primary hydration shell. Most of these calculations resulted in an immediate rearrangement of the water molecules with some ligands moving out of the first hydration shell. Only the calculation with symmetry restriction could yield a final structure with eight water molecules bound to the copper (**6d**). This structure is, however, 285 kJ/mol above the lowest energy structure (**6a**). The most favored structure (**6a**), on the other hand, has only four water molecules in the first hydration shell, and all four other water molecules are double-hydrogen-bonded to the primary shell water molecules. In this structure the number of hydrogen bonds is maximized with four primary

hydration shell water molecules, and this structure is strongly favored in terms of energy over other possibilities. The energetic cost of moving one water from the second layer to the axial position (**6c**) is 23 kJ/mol.

Most of the structures described in this section were determined by a combination of static and dynamical density functional theory calculations. We demonstrate on an eight-coordinated structure how we found the most stable conformation by dynamical simulations. The dynamics trajectory started from a structure with all eight water molecules in the primary hydration shell (**6d**) and converged to the conformation corresponding to the most stable conformation (**6a**) in 10 ps simulations. Normally, a 10 ps simulation time is too short to find stable geometries significantly different from the original starting conformation. In this case, however, the energetic preference for the lowest energy conformation is so significant that the final conformation is reached relatively quickly. Starting the dynamics from a high-energy conformation also ensured that the trajectory did not get stuck in a local minimum on the potential surface. Figure 3 shows the evolution of hydrogen bond length as a function of simulation time during the dynamics of $[\text{Cu}(\text{H}_2\text{O})_8]^{2+}$ starting from the high-energy structure with eight water molecules in the primary hydration shell. The final structure with a total of eight hydrogen bonds is reached in 10 ps. When the dynamics was started from different conformations, the trajectory did not always reach the most stable structure within the 10 ps simulation time. For example, starting the dynamical trajectory from the axially bonded conformation

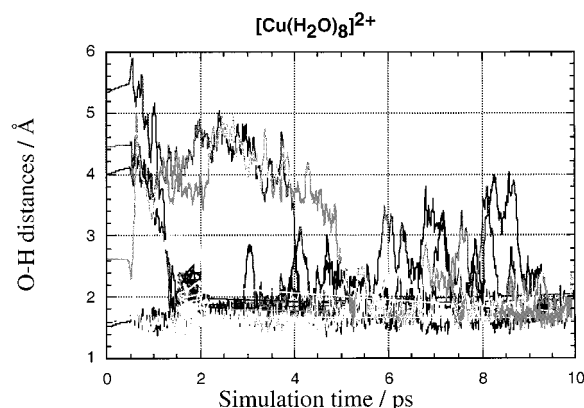


Figure 3. Evolution of hydrogen bond in dynamical simulation.

(6c) did not reach the lowest energy conformation in 10 ps. Most likely there is a significant barrier between the axially bound and the hydrogen-bonded conformations.

As these and previous examples from the literature show, the energetic preferences of metals for one particular solvation configuration is often very strong. For this reason, *ab initio* molecular dynamics may be the ideal way to study the structures of these clusters. In the case of a high-energy conformation, the trajectory could lead to a more stable structure within a short simulation time. If the structure does not change drastically in the first few picoseconds of the dynamical simulation, other structural alternatives have to be tested. Another example of a structure that was found by analyzing the dynamical trajectories is the cluster with seven water molecules with one water partly hydrogen-bonded and partly axially bonded (5b). Such structures may represent a transition state of moving the axial ligand into the second hydration shell.

During the construction of the initial structures with ammonia as a solvent, we started from the structure with water and replaced one of the lone pairs with hydrogen atoms. This strategy has worked remarkably well for all structures without a solvent molecule in the second solvation shell. The structures without secondary ammonia are remarkably similar to their water-solvated analogues. The Cu^{2+} cluster with three ammonia solvent assumes a trigonal planar conformation with significant distortion from the ideal triangle (7a) with the largest N—Cu—N bending angle of 158° . The Cu—N bonds are 1.97 and 2.03 Å, which is longer than the Cu—O bond in the water analogue. On the other hand, the average binding energy of ammonia is 478 kJ/mol, which is 100 kJ/mol above that of water in the analogous cluster.

Four ammonia molecules prefer to bind to Cu^{2+} in a distorted planar tetragonal geometry (8a–8f). The distortion toward tetrahedral geometry is similar to that of the water analogue with a typical trans N—Cu—N bending angle of 166 – 168° . We found six different structures within 6 kJ/mol energy separation, which is a further indication that the potential number of different conformations is large. The separation between different conformations was more significant in the case of the water solvent, which has an electron pair that does not participate in the bonding. As a significant difference between water and ammonia, $[\text{Cu}(\text{NH}_3)_4]^{2+}$ prefers nonplanar conformations while $[\text{Cu}(\text{H}_2\text{O})_4]^{2+}$ prefers planar ones. Although one of the conformations (8e) is essentially planar, it is likely to be a transition state between two nonplanar structures.

The fifth ammonia molecule can assume the axial position of the tetragon (9b) or it can be hydrogen-bonded to one of the ammonia in the first hydration shell (9a). Since ammonia has

only one lone pair as opposed to water, which has two, it cannot form two strong hydrogen bonds to two ammonia molecules in the first hydration shell. Despite this difference, the structure with two hydrogen bonds connecting the secondary ammonia to the primary solvation shell (9a) gives the most stable structure similarly to the analogous water cluster. However, the tetragonal pyramidal structure with the fifth ammonia in the axial position (9b) is only 2 kJ/mol above the most stable structure. The sequential binding energies of the fifth ammonia in the hydrogen-bonded and axial positions are 97 and 95 kJ/mol, respectively. Thus, the axial binding energy to $[\text{Cu}(\text{NH}_3)_4]^{2+}$ is of comparable strength to that of the hydrogen bond. A trigonal bipyramidal structure (9c), which is likely to be the transition state between two equivalent tetragonal pyramidal structures, is within 0.5 kJ/mol in energy compared to the tetragonal pyramid (9b). The close energetics of these structures suggest the possibility of a fluxional behavior with the axial and equatorial ammonia constantly changing positions.

The ammonia in the second hydration shell can be either bonded with a single hydrogen bond to one primary ligand (9d) or with two hydrogen bonds to two primary ligands (9a). The length of the single hydrogen bond is 1.78 Å, whereas those in the double-hydrogen-bonded structures are 1.98 and 2.05 Å. The single-hydrogen-bonded structure is only 4 kJ/mol above the energy of the double-hydrogen-bonded structure, indicating a comparable strength for the single and the double hydrogen bonds. This is a significant difference from water, which has two lone pairs and a strong energetic preference to form two hydrogen bonds.

The most stable structure of $[\text{Cu}(\text{NH}_3)_6]^{2+}$ has a planar tetragonal primary hydration shell with two ammonia molecules doubly hydrogen-bonded to it (10a). The two ammonia molecules in the second hydration shell are on opposite sides of the tetragon. This is different from the water analogue, which shows a preference for binding the two water molecules on the two adjacent sides (i.e., 4a). The energetic difference, however, is not very significant, only 6 kJ/mol between these two most stable structures (10a and 10b). The sequential binding energy in the doubly hydrogen-bonded position of the most stable structure is 95 kJ/mol, which is only 6 kJ/mol stronger than binding in the axial position (10c). The energetic preference for the hydrogen bond and axial binding is similar to that in the five-coordinated clusters. We found two alternatives for the octahedral structures: one with long axial (2.48 and 2.90 Å) and short equatorial (2.09–2.10 Å) bonds (10d) and another with short axial (2.06 Å) and long equatorial (2.35–2.39 Å) bonds (10e). The former is lower in energy by 66 kJ/mol and has a sequential binding energy of 58 kJ/mol. These results suggest that the binding energy of the first axial position is stronger than the second one, which is also reflected in the large inequality in the Cu—N bond length in the axial position (10d).

The most stable conformation of $[\text{Cu}(\text{NH}_3)_6]^{2+}$ has a quasi-planar structure with four ammonia molecules in the primary hydration shell (11a). The corresponding sequential binding energy is 76 kJ/mol. The second most stable structure is based on a tetragonal pyramidal core with two ammonia molecules single-hydrogen-bonded to two equatorial ligands (11b). The second solvation shell molecules are far out-of-plane of the equatorial ligands. Those structures that have the secondary solvent molecules in quasi-planar positions (11c–11d) are significantly higher in energy. The highest energy conformation is based on the octahedral primary solvation shell.

The analogous water and ammonia clusters with eight solvent molecules around Cu^{2+} are similar in their preference for a

quasiplanar structure with primary and secondary solvation shells of four solvent molecules in both **6a** and **12a**. The difference lies in the energetic cost of moving one solvent from the hydrogen-bonded position to the axial position, which is 5 kJ/mol for the ammonia cluster (**12a** to **12b**) but 23 kJ/mol for the water clusters (**6a** to **6b**). This is consistent with the general trend that ammonia has similar bond strength in the axial and hydrogen-bonded positions, while water has a strong preference for hydrogen bonds. Partial symmetrization of **12a** yields **12c**, which is 10 kJ/mol higher in energy. The conformation with octahedral core (**12d**) is 89 kJ/mol above the most stable structure. The structure with eight water molecules in the first solvation shell (**12e**) has very high energy.

Discussion

The nature of the stationary points of structures obtained by geometry optimization is not always known, but most likely, the majority of the structures described here are minima on the potential surface. However, some structures have features indicative of a transition state, like the trigonal bipyramidal conformation of $[\text{Cu}(\text{NH}_3)_5]^{2+}$ (**9c**), which seems to connect the ligand exchange between the first and second hydration shells of “4 + 1” structures. We have studied water exchange between the first and second hydration shell by constrained ab initio molecular dynamics of $[\text{Cu}(\text{H}_2\text{O})_8]^{2+}$ and found that the transition state of water exchange has a trigonal bipyramidal core. This confirms that **9c** is a probable transition state associated with the solvent exchange process. The structure in which one of the water molecules is partly bonded axially to the metal and partly hydrogen-bonded to the first solvation shell (**5b**) is also a likely candidate for a transition state for the ligand exchange process. In this case, however, this is an exchange of the position of one ligand from the primary to the secondary solvation shell, as opposed to the previous process that involves the exchange of two ligands between the primary and secondary solvation shells.

These clusters are likely to have several dozen different conformations depending on the relative orientation of the ligands. It is possible that the structures we found do not always represent the lowest energy structures. However, the major determining factors of the solvation energies are (i) the number of primary ligands, (ii) the number of axial bonded ligands, and (iii) the number of hydrogen bonds. The binding energies of both the axial and hydrogen-bonded positions show a consistent trend throughout the series of clusters. For this reason, our limited set of clusters is a consistent representation of the different types of bonding and gives a good basis for assessment for the binding energies.

The strength of the hydrogen bond is likely to be somewhat overestimated by density functional theory. However, the preference for the hydrogen bond over axial binding is so strong in the case of water that such a preference cannot be an artifact of DFT methods. It is not as clear in the case of ammonia, which has only a minor preference for the hydrogen bond over the axial position. Water prefers the hydrogen-bonded position in Cu(II) –water clusters by about 20–35 kJ/mol compared to the axial position throughout the cluster series, as opposed to ammonia, which shows the analogous preference by only a few kJ/mol. The difference between axial and equatorial binding energies is consistent with the d^9 electron configuration where the unpaired electron occupies the antibonding $d_{x^2-y^2}$ orbital.

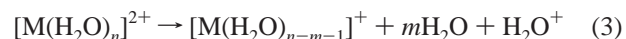
The binding energy of the axial ligand to Cu(II) is stronger than the hydrogen bond between water or ammonia molecules in solution but weaker than the hydrogen bond connecting the

first and second solvation shell and much weaker than the equatorial binding energy. Consequently, in solution phase, the axial position is occupied and the solvated Cu(II) ions have a distorted octahedral core with fluxional axis orientation. Therefore, the usual formulas of $[\text{Cu}(\text{H}_2\text{O})_6]^{2+}$ and $[\text{Cu}(\text{NH}_3)_6]^{2+}$ correctly describe the first solvation shell in solution. As this example shows, the gas-phase shell development does not reflect properly the structure of the solvation shell in solution phase when only a limited number of solvent molecules are considered.

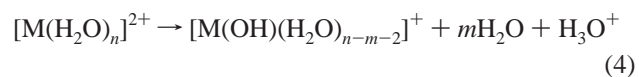
Water has a strong preference in the second hydration shell to be bound to two water molecules of the primary shell. For ammonia, the strength of one or two hydrogen bonds is comparable and the double-hydrogen-bonded structure is preferred only by a few kJ/mol. This difference between water and ammonia is understandable, since water has two lone pairs while ammonia has only one. In fact it is surprising that ammonia can build two hydrogen bonds in a bridging position with only one lone pair. Tuckerman and co-workers reported a similar situation related to the ab initio simulation of proton transfer in water.⁴⁸ They found that OH^- prefers to be hydrogen-bonded to four water molecules despite the number of lone pairs being only three.

In terms of preference between oxygen and nitrogen donors, Cu^{2+} has a clear preference for nitrogen coordination. This is consistent with the fact that Cu prefers to be coordinated to the nitrogen donor histidine or to sulfur donor cysteine in enzymes.⁴⁹ Although copper is coordinated to an oxygen donor, glutamic acid, in azurines, the binding of oxygen ligands to copper is usually a reversible process. In fact, copper plays a significant role in the reversible binding of dioxygen as an oxygen carrier in hemocyanin or in the catalytic activation of dioxygen in tyrosinase or multicopper oxidases.⁴⁹ These functions require that oxygen-based substrates can bind reversibly to copper, which can be achieved only if copper has only a modest affinity to bind oxygen donors.

Our original quest was to explain the maximum ion intensity in the MS spectrum of divalent copper water clusters at eight solvent molecules.^{11,12} The factors that contribute to the intensity are (i) the instability of smaller clusters with respect to electron transfer from the solvent to the metal and (ii) the natural decline in intensity that is common to most cluster distributions as a function of cluster size. From the consideration of the experimental circumstances it is clear that the abundance in the mass spectrum is not correlated to thermodynamic stability but rather to the kinetic stability of the clusters. The most important consideration is the electron-transfer-induced fragmentation processes



and



It is not feasible to calculate the barrier of electron transfer between the ligand and the metal, which would give insight into the reasons for the high kinetic stability of $[\text{Cu}(\text{H}_2\text{O})_8]^{2+}$ and $[\text{Cu}(\text{NH}_3)_8]^{2+}$. However, we find a correlation between the geometry of the first solvation shell of the most stable conformation and the ion signal. The hydrogen bond network of the most stable conformations of $[\text{Cu}(\text{H}_2\text{O})_8]^{2+}$ and $[\text{Cu}(\text{NH}_3)_8]^{2+}$ stabilizes the quasiplanar geometry of the primary solvation shell. Planarity can be measured by the dihedral angles of the four primary solvation shell ligands or that defined

between three ligands and the central atom. It is absolutely remarkable that the largest deviation from the plane measured by these dihedral angles is 0.7° and 0.2° for $[\text{Cu}(\text{H}_2\text{O})_8]^{2+}$ and $[\text{Cu}(\text{NH}_3)_8]^{2+}$, respectively. By contrast, the most stable conformation of $[\text{Cu}(\text{NH}_3)_4]^{2+}$ is significantly distorted from the plane and characterized by a dihedral angle of about 20° . Both $[\text{Cu}(\text{NH}_3)_4]^{2+}$ and $[\text{Cu}(\text{H}_2\text{O})_4]^{2+}$ prefer to distort from the 4-fold symmetric structure. However, $[\text{Cu}(\text{H}_2\text{O})_4]^{2+}$ can distort within the plane without energetic penalty, while a similar distortion of $[\text{Cu}(\text{NH}_3)_4]^{2+}$ is less favorable. For this reason, $[\text{Cu}(\text{NH}_3)_4]^{2+}$ adopts a nonplanar geometry in its most stable conformation while $[\text{Cu}(\text{H}_2\text{O})_4]^{2+}$ adopts a planar geometry in its most stable conformation. This finding is consistent with the experimental ion intensity pattern, which shows a local maximum at $[\text{Cu}(\text{H}_2\text{O})_4]^{2+}$ but does not indicate any significant stability for $[\text{Cu}(\text{NH}_3)_4]^{2+}$. Therefore, the planar primary solvation shell of $[\text{Cu}(\text{NH}_3)_8]^{2+}$ is not an inherent property of the $[\text{Cu}(\text{NH}_3)_4]^{2+}$ core but stabilized by the network of hydrogen bonds.

Conclusions

The combination of static and dynamic density functional theory is an efficient way to find energetically significant conformations of metal–solvent clusters in the gas phase. We were particularly pleased to find the most stable conformation of $[\text{Cu}(\text{H}_2\text{O})_8]^{2+}$ from a very unreasonable starting structure within a short 10 ps simulation. These calculations suggest that water has an energy preference of about 20–35 kJ/mol to be bound through hydrogen bonds to the primary solvation shell as opposed to occupying the axial position of a planar tetragonal structure. Ammonia also prefers the hydrogen bond over the axial position, but the energetic preference is only a few kJ/mol. Water in the second hydration shell prefers to form two hydrogen bonds with the two lone pairs connecting to two adjacent primary ligands. It is remarkable that ammonia with only one lone pair can also be involved in two hydrogen bonds, but the preference for such a double hydrogen bond is only a few kJ/mol relative to a single hydrogen bond. The network of hydrogen bonds in the most stable structures of $[\text{Cu}(\text{H}_2\text{O})_8]^{2+}$ and $[\text{Cu}(\text{NH}_3)_8]^{2+}$ impose a planar geometry on the primary solvation shell, which gives high kinetic stability to these systems.

Acknowledgment. The authors thank Peter Blöchl for the use of the PAW program and for valuable comments on the manuscript. We also thank Tom K. Woo for assistance with the PAW. Access to computational resources from the Japan Science and Technology Corporation is gratefully acknowledged.

References and Notes

- (1) Greenwood, N. N.; Earnshaw, A. *Chemistry of the Elements*; Pergamon: Oxford, 1984; Chapter 5.
- (2) Babu, Y. S.; Sack, J. S.; Geenough, T. J.; Bugg, C. E.; Means, A. R.; Cook, W. J. *Nature* **1985**, *315*, 37–40.
- (3) Weis, W. I.; Drickamer, K.; Hendrickson, W. A. *Nature* **1992**, *360*, 127–134.
- (4) Katz, A. K.; Glusker, J. P.; Beebe, S. A.; Bock, C. W. *J. Am. Chem. Soc.* **1996**, *118*, 5752–5763.
- (5) (a) Bock, C. W.; Glusker, J. P. *Inorg. Chem.* **1993**, *32*, 1242–1250. (b) Sánchez Marcos, E.; Pappalardo, R. R.; Rinaldi, D. *J. Phys. Chem.* **1991**, *95*, 8928–8932.
- (6) Bock, C. W.; Kaufman, A.; Glusker, J. P. *Inorg. Chem.* **1994**, *33*, 419–427.
- (7) Bock, C. W.; Katz, A. K.; Glusker, J. P. *J. Am. Chem. Soc.* **1995**, *117*, 3754–3765.
- (8) Lee, S.; Kim, J.; Park, J. K.; Kim, K. S. *J. Phys. Chem.* **1996**, *100*, 14329.
- (9) Kim, K. S.; Lee, S.; Mhin, B. J.; Cho, S. J.; Kim, J. *Chem. Phys. Lett.* **1993**, *216*, 309–312.
- (10) Rodriguez-Cruz, W. E.; Jockusch, R. A.; Williams, E. R. *J. Am. Chem. Soc.* **1998**, *120*, 5842–5843.
- (11) Stace, J. A.; Walker, N. R.; Firth, S. J. *Am. Chem. Soc.* **1997**, *119*, 10239–10240.
- (12) Walker, N. R.; Firth, S.; Stace, A. J. *Chem. Phys. Lett.* **1998**, *292*, 125–132.
- (13) Woodward, C. A.; Dobson, M. P.; Stace, A. J. *J. Phys. Chem.* **1996**, *100*, 5605.
- (14) Dobson, M. P.; Stace, A. J. *J. Chem. Soc., Chem. Commun.* **1996**, 1533.
- (15) Dobson, M. P.; Woodward, C. A.; Stace, A. J. *J. Phys. Chem. A* **1997**, *101*, 2279.
- (16) Dobson, M. P.; Stace, A. J. *Int. J. Mass Spectrom. Ion Processes*, in press.
- (17) Cooks, R. G.; Beynon, J. H.; Caprioli, R. M.; Lester, G. R. In *Metastable Ions*; Elsevier: Amsterdam, 1973.
- (18) Cotton, F. A.; Wilkinson, G. W. In *Advanced Inorganic Chemistry*; Wiley: London, 1988.
- (19) Car, R.; Parrinello, M. *Phys. Rev. Lett.* **1985**, *55*, 2471.
- (20) Ramaniah, L. M.; Bernasconi, M.; Parrinello, M. *J. Chem. Phys.* **1998**, *109*, 6839.
- (21) Brugé, F.; Bernasconi, M.; Parrinello, M. *J. Chem. Phys.* **1999**, *110*, 4734.
- (22) Deng, Z.; Klein, M. L.; Martyna, G. J. *J. Chem. Soc., Faraday Trans.* **1994**, *90*, 2009.
- (23) Deng, Z.; Martyna, G. J.; Klein, M. L. *J. Chem. Phys.* **1994**, *100*, 7590.
- (24) Baerends, E. J.; Ellis, D. E.; Ros, P. *Chem. Phys.* **1973**, *2*, 41.
- (25) Ravenek, W. In *Algorithms and Applications on Vector and Parallel Computers*; te Riele, H. J. J., Dekker, Th. J., van de Vorst, H. A., Eds.; Elsevier: Amsterdam, 1987.
- (26) Boerrigter, P. M.; te Velde, G.; Baerends, E. J. *Int. J. Quantum Chem.* **1988**, *33*, 87.
- (27) te Velde, G.; Baerends, E. J. *J. Comput. Phys.* **1992**, *99*, 84.
- (28) Fan, L.; Ziegler, T. *J. Chem. Phys.* **1991**, *94*, 6057.
- (29) Fan, L.; Ziegler, T. *J. Chem. Phys.* **1991**, *95*, 7401.
- (30) Fan, L.; Versluis, L.; Ziegler, T.; Baerends, E. J.; Ravenek, W. *Int. J. Quantum Chem.* **1988**, *S22*, 173.
- (31) Fan, L.; Ziegler, T. *J. Chem. Phys.* **1992**, *96*, 9005.
- (32) Fan, L.; Ziegler, T. *J. Phys. Chem.* **1992**, *96*, 6937.
- (33) Vosko, S. H.; Wilk, L.; Nusair, M. *Can. J. Phys.* **1980**, *58*, 1200.
- (34) Becke, A. D. *Phys. Rev. A* **1988**, *38*, 2398.
- (35) Perdew, J. P. *Phys. Rev. B* **1986**, *33*, 8822; **1986**, *B34*, 7046.
- (36) (a) Snijders, J. G.; Baerends, E. J.; Ros, P. *Mol. Phys.* **1978**, *36*, 1789. (b) Snijders, J. G.; Baerends, E. J.; Ros, P. *Mol. Phys.* **1979**, *36*, 1969.
- (37) Schreckenbach, G.; Ziegler, T.; Li, J. *Int. J. Quantum Chem.* **1995**, *56*, 477.
- (38) (a) Snijders, G. J.; Baerends, E. J.; Vernooijs, P. *At. Data Nucl. Data Tables* **1982**, *26*, 483. (b) Vernooijs, P.; Snijders, G. J.; Baerends, E. J. *Slater Type Basis Functions for the Whole Periodic System*; Internal Report; Free University of Amsterdam: The Netherlands, 1981.
- (39) Krijn, J.; Baerends, E. J. *Fit functions in the HFS-method* (in German); Internal Report; Free University of Amsterdam, The Netherlands, 1984.
- (40) Ziegler, T. *Chem. Rev.* **1991**, *91*, 651.
- (41) Blöchl, P. E. *Phys. Rev. B* **1994**, *50*, 17953.
- (42) Carloni, P.; Blöchl, P. E.; Parrinello, M. *J. Phys. Chem.* **1995**, *99*, 1338–1348.
- (43) Perdew, J. P.; Zunger, A. *Phys. Rev. B* **1981**, *23*, 5048.
- (44) Blöchl, P. E. *J. Chem. Phys.* **1995**, *103*, 7422.
- (45) Hoover, W. G. *Phys. Rev. A* **1985**, *31*, 1695.
- (46) Nosé, S. *Mol. Phys.* **1984**, *52*, 255.
- (47) Blöchl, P. E.; Parrinello, M. *Phys. Rev. B* **1992**, *45*, 9413.
- (48) Tuckerman, M.; Laasonen, K.; Sprk, M. *J. Chem. Phys.* **1995**, *103*, 150–161.
- (49) Holm, R. H.; Kennepohl, P.; Solomon, E. I. *Chem. Rev.* **1996**, *96*, 2239–2314.